

A survey of the structural models proposed for $\text{PbZr}_{1-x}\text{Ti}_x\text{O}_3$ using mode analysis

Balazs Kocsis,^{a*} J. M. Perez-Mato,^b Emre S. Tasci,^c Gemma de la Flor^b and Mois I. Aroyo^b

^aCrystallography Section, Ludwig-Maximilians Universität München, Germany, ^bDepartamento de Física de la Materia Condensada, Facultad de Ciencia y Tecnología, Universidad del País Vasco (UPV-EHU), Bilbao, Spain, and ^cDepartment of Physics, Middle East Technical University (METU), 06800 Ankara, Turkey. Correspondence e-mail: b.kocsis@lmu.de

The numerous structures that have been reported for the different phases of the lead zirconate titanate system, $\text{PbZr}_{1-x}\text{Ti}_x\text{O}_3$ (PZT), are analysed by means of a systematic symmetry-mode analysis. The distortion corresponding to the order parameter has been separated out and expressed in all phases in a comparable form. The fact that the physical origin of the PZT phases is an unstable threefold degenerate polar mode, plus in some cases an unstable octahedral tilting mode, produces structural correlations between the different phases. These correlations had remained unnoticed until now but are directly observable in a mode parameterization. They can be used both to characterize the evolution of the order parameters through the phase diagram and as a stringent test of the reported structural models. It is further shown that the activity of a single polar mode yields a specific feature in the mode decomposition of the monoclinic phases. This single-mode signature can be observed in the majority of the monoclinic structures proposed, making the others questionable. In fact, this internal constraint is satisfied by PZT to such a high degree that it drastically reduces the number of effective structural degrees of freedom. It is conjectured that this type of structural constraint beyond space-group symmetry can be a rather general property of low-symmetry distorted structures. As shown here, its existence can be detected and assessed by a symmetry-mode analysis, if considered in relation to the single underlying multidimensional order parameter.

© 2014 International Union of Crystallography

1. Introduction

The solid solution $\text{PbZr}_{1-x}\text{Ti}_x\text{O}_3$ (PZT) is a ferroelectric material widely used because of its competitive functional properties, in particular its piezoelectric and pyroelectric response (Lines & Glass, 1977). The instability of a polar mode of its high-temperature cubic perovskite phase, analogous to that present in pure PbTiO_3 , is the driving agent of its distorted phases. Its phase diagram is rather complex, with competing phases that result from different directions taken by the unstable polar order parameter, combined in some phases with a tilting mode of the oxygen octahedra (Woodward *et al.*, 2005; Frantti, 2008). The region around $x = 0.5$ is of particular interest because there the piezoelectric response reaches its highest values (Jaffe *et al.*, 1971). Many structural models of the various phases have been reported [see Frantti (2008) for a review], especially in this middle composition range where two low-symmetry monoclinic phases have been observed, their existence being related to the significant increase in piezoelectricity in this composition range.

The advantages of the application of a symmetry-mode decomposition in the analysis of ferroic materials, and of

distorted structures in general, have been stressed recently (Perez-Mato *et al.*, 2010). Symmetry-mode analysis allows a quantitative comparison of different structural models, separating out the effects of different distortion mechanisms. Variations in the amplitudes of the distortion modes are separated from changes in their internal forms and are quantitatively described by the so-called 'polarization vector', a normalized mode that defines the specific linear combination of atomic displacements (basis symmetry modes) involved in the distortion. The relative contribution of different atomic displacements within a distortion mode is expected to be weakly dependent on both temperature and composition. This implies similar mode polarization vectors for structures obtained under different conditions, while the main variations are expected to occur in their global amplitudes.

In this context we report a systematic symmetry-mode analysis of most of the reported structures of PZT. Both amplitudes and polarization vectors of the distortion modes, describing the structures observed at different temperatures, compositions and phases, are studied in detail. The various phases of PZT arise, in agreement with Landau theory, from a

common structural threefold degenerate instability of the high-symmetry parent phase. We show here that, in this situation (rather common to many materials), the symmetry-mode parameterization can be extended and used to analyse and compare structures with different symmetries. The fact that the unstable mode transforms according to a single three-dimensional irreducible representation (irrep) of the parent space group is shown to produce stringent structural correlations, which are detected using a symmetry-mode parameterization. This allows a quantitative characterization of the underlying order parameter. Hence, it should be stressed that the uncertainties in the published structural models of PZT (obtained from powder diffraction) are expected to be high, especially in the case of the monoclinic phases, because of the considerable number of positional parameters and their high pseudo-symmetry. Their description in terms of modes, presented here, allows a direct comparison with the neighbouring or coexisting rhombohedral phases and a quantitative assessment of the variation of the order parameter between phases. By this means, physically inconsistent features in some of the published models will be pointed out. Furthermore, in the case of the monoclinic phases of PZT, it will be shown that the prevalence of a single driving mode is bound to introduce strong structural correlations, which are beyond conventional space-group constraints. These correlations are indeed fulfilled to a very good approximation by the majority of the published monoclinic structures, and their evaluation enables the determination of the direction of the order parameter, which in principle is composition- and temperature-dependent. In fact, we will demonstrate that this single-mode structural signature is satisfied to such a high degree that it could be used to reduce the number of effective parameters characterizing the monoclinic phases of PZT. The argument explaining this property is very general, and therefore the existence of specific structural signatures associated with the prevalence of a single multidimensional order parameter should be expected to be a rather general property in low-symmetry distorted structures. They could be detected and assessed if the structures were described in terms of distortion modes and considered in relation to the underlying order parameter. The presence of single-order-parameter constraints or restraints in a symmetry-mode description, demonstrated in this work, opens up a novel approach in the study of the structural properties of ferroic materials (and distorted structures in general) of very low symmetry.

As precursor to the present study, one should cite the work of Hatch *et al.* (2002), who analysed under the mode perspective the monoclinic *Cc* phase of PZT in order to justify the assignment of this symmetry. However, to the best of our knowledge, a comprehensive mode analysis of the phases of PZT has never been reported. It is important to stress that the analysis presented here is performed on average structures. The distortion modes with respect to the cubic perovskite configuration are therefore defined in terms of displacements in the average positions of the atoms. This is especially important in this material, where the Zr and Ti cations are disordered and occupy a common average site with a frac-

tional occupancy. It is not at all to be taken for granted that, in such cases, a description of the distorted average structures in terms of displacive modes (involving the disordered mixed sites as a single site) could reflect the basic physical mechanism underlying the stabilization of these distorted phases. However, the results of the analysis discussed in this work show that this is indeed the case. Despite the intrinsic disorder represented by the partially occupied Zr/Ti mixed sites, the mode decomposition of the structures shows that a specific single threefold degenerate polar mode involving these mixed sites underlies all the observed phases.

It is also important to remark that the mode analyses and structure comparisons in terms of modes that are presented here do not include lattice strains. The structural distortion relating the parent and distorted phases can be deconvoluted into changes in the atomic positions within the lattice unit cell measured in relative units, plus a strain in this unit cell. Displacive modes refer to the former, and their translation in absolute length values is done using an unstrained lattice (Orobengoa *et al.*, 2009; Perez-Mato *et al.*, 2010).

2. Method

Structural data were retrieved from the Inorganic Crystal Structure Database (ICSD, January 2013 release; FIZ-Karlsruhe, <http://icsd.fiz-karlsruhe.de/>). More than 80 reported structures were decomposed and analysed in terms of modes using the program *AMPLIMODES* (Orobengoa *et al.*, 2009) of the Bilbao Crystallographic Server (BCS; Aroyo, Perez-Mato *et al.*, 2006; Aroyo, Kirov *et al.*, 2006; Aroyo *et al.*, 2011). The positions in the phase diagram of the different structures

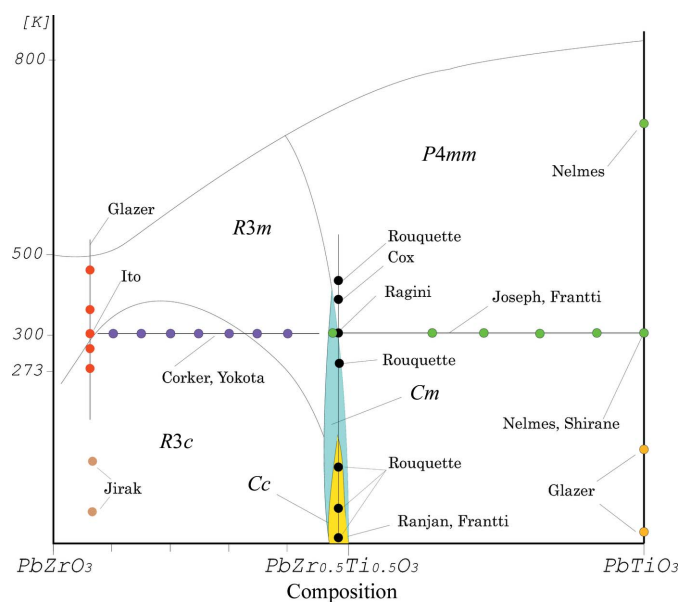


Figure 1 Scheme of the phase diagram of PZT, showing the approximate locations of the various structural models that have been reported to date and are analysed in this work. The border lines are only approximate guides to define the prevailing phase in each region. In some cases, the structures have been derived assuming the coexistence of two or more phases over wide intervals of composition. The phases appearing for compositions close to pure PbZrO_3 are not shown.

Table 1

Unit-cell transformations with respect to the parent $Pm\bar{3}m$ structure used for the different structures reported for PZT.

The origin shift is also indicated. Only one of the possible equivalent choices is given. All the symmetry-mode analyses reported here have been done with these transformations and using, as a common parent reference cubic structure, that of PZT ($x = 0.10$) (Yokota *et al.*, 2011) at high temperature, with a cell parameter of 4.145 Å and the cell origin at the Pb site.

Phase symmetry	Transformation matrix
$P4mm$	$(a, b, c; 0, 0, 0)$
Cm	$(a - b, a + b, c; 0, 0, 0)$
Cc	$(a - b + 2c, a + b, -a + b; \frac{1}{4}, \frac{1}{4}, 0)$
$R3c$	$(-b + c, a - c, 2a + 2b + 2c; \frac{1}{2}, \frac{1}{2}, \frac{1}{2})$

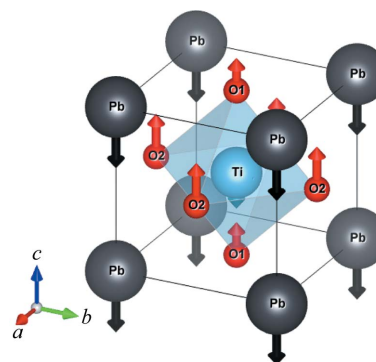
studied are indicated in Fig. 1. The high-temperature $Pm\bar{3}m$ structure ($a = 4.145$ Å) reported by Yokota *et al.* (2011) for $x = 0.10$ has been used as the common reference parent structure for the mode decomposition of all the structures. The origin was chosen such that the mixed Zr/Ti site is at $(\frac{1}{2}, \frac{1}{2}, \frac{1}{2})$. It should be noted that the irrep label for the relevant modes depends on this origin choice. The explanation for this variation, and the irrep label equivalences when choosing the origin at the Zr/Ti site, can be found in Appendix A. The transformations to the settings used for the different phases are listed in Table 1. This implies an arbitrary choice made among possible different (but equivalent) relations between the cubic parent space group and the space group of the distorted phase. This multiplicity of equivalent transformations corresponds to domain-related equivalent descriptions of the distorted structure with respect to the cubic parent phase, and a fixed choice is introduced so that the different structures, when described in terms of distortion modes, are directly comparable. Some structural models in the database are given in other settings, but they were transformed to a setting consistent with Table 1 by means of a convenient change in the unit cell and/or an origin shift. These necessary transformations were easily determined by means of the BCS tools *COMPSTRU* (<http://www.cryst.ehu.es/cryst/compstru.html>) and *SETSTRU* (<http://www.cryst.ehu.es/cryst/setstru.html>).

3. Tetragonal $P4mm$ phase of $PbTiO_3$

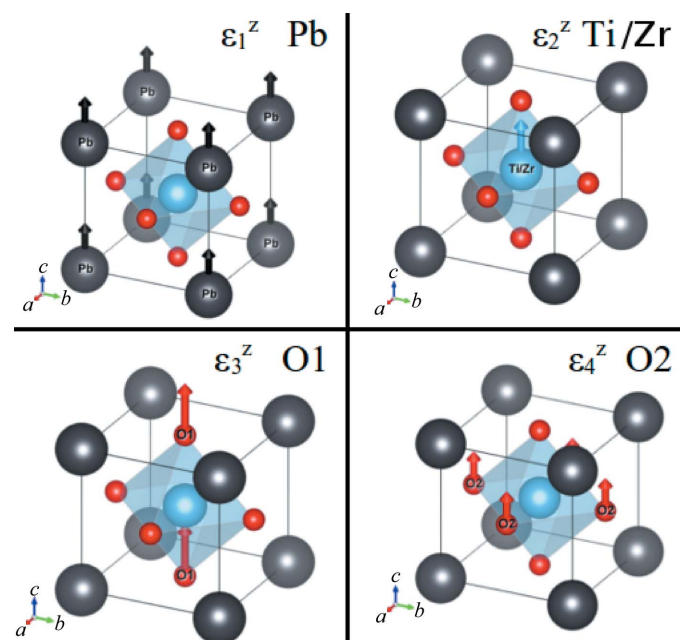
Let us first consider the tetragonal $P4mm$ phase of pure lead titanate. This phase is the result of the condensation of a polar mode along z (Lines & Glass, 1977; Ghosez *et al.*, 1999), which transforms according to the three-dimensional irrep $GM4^-$ of $Pm\bar{3}m$ [the irrep labels are those used by the software *ISOTROPY* (Stokes *et al.*, 2007)]. The form of the frozen $GM4^-$ mode observed in the tetragonal phase of $PbTiO_3$ is represented schematically in Fig. 2. A distortion of this type can be described as a linear combination of a set of four normalized basis modes, $\{\varepsilon_1^z, \varepsilon_2^z, \varepsilon_3^z, \varepsilon_4^z\}$, with displacements directed along the z axis (see Fig. 3 and its caption). In the following, we order these basis modes in the form shown in Fig. 3, namely modes 1 and 2 correspond to the Pb and Zr/Ti sites, respectively, while modes 3 and 4 correspond to the apical and basal O atoms, respectively. Following Perez-Mato *et al.* (2010) and Orobengoa *et al.* (2009), the normalization of

these basis modes is chosen such that the square root of the sum of the squares of all atomic displacements within a unit cell is 1 Å, and this is done in the metric defined by the unit cell of the cubic structure used as reference. Each one of these four basis modes along z , together with its analogous ones along x and y , forms triplets, $\{\varepsilon_i^x, \varepsilon_i^y, \varepsilon_i^z\}$, which transform according to the above-mentioned three-dimensional irrep $GM4^-$. Obviating the strain (which can be considered separately), one can describe a $P4mm$ structural distortion Qe^z with respect to the perovskite as

$$Qe^z = Q(c_1\varepsilon_1^z + c_2\varepsilon_2^z + c_3\varepsilon_3^z + c_4\varepsilon_4^z), \quad (1)$$

**Figure 2**

Relative atomic displacements, with respect to the cubic structure, that take place in the $P4mm$ phase of $PbTiO_3$ and define its polar distortion mode.

**Figure 3**

The four basis symmetry modes present in a polar distortion of the perovskite structure along z . The 12-dimensional subspace of all possible polar distortions is spanned by this set of basis modes, plus analogous sets along x and y . Note that, while the first three modes involve a single atom per unit cell, the mode ε_4^z involves two atoms per cell, and therefore the normalization condition implies that the atomic displacements in this fourth basis mode are smaller by a factor of $1/2^{1/2}$.

Table 2

$P4mm$ structural models of PbTiO_3 , according to various experimental reports or first-principles calculations.

The structures are parameterized in terms of the amplitude of the polar distortion mode and the components of its mode polarization vector, as described in the text. The similarity of the distortion modes is checked through the scalar product of their polarization vector with that of Nemes & Kuhs (1985) at 298 K (entry 1), which is taken as reference. The cases where no amplitude is indicated are *ab initio* calculations of the unstable polar phonon mode in the cubic structure. The numbers in the ICSD column are deposition codes in the Inorganic Crystal Structure Database. In the Technique column, NSD denotes neutron single-crystal diffraction, NPD neutron powder diffraction and XPD X-ray powder diffraction.

Entry	ICSD	Source	Technique	Temperature (K)	Mode amplitude (Å)	Normalized polarization vector				$\mathbf{e}(61168) \cdot \mathbf{e}$
						c_1	c_2	c_3	c_4	
1	61168	(a)	NSD	298	0.453 (1)	−0.703 (3)	−0.358 (5)	0.320 (5)	0.525 (8)	1
2	61169	(a)	NSD	700	0.323 (1)	−0.691 (3)	−0.376 (5)	0.317 (5)	0.530 (8)	1.00
3	1610	(b)	NPD	90	0.469	−0.707	−0.354	0.336	0.512	1.00
4	1611	(b)	NPD	158	0.463	−0.712	−0.345	0.316	0.523	1.00
5	1612	(b)	NPD	298	0.443 (7)	−0.71 (1)	−0.35 (2)	0.33 (2)	0.51 (3)	1.00
6	16621	(c)	NSD	298	0.43 (2)	−0.72 (4)	−0.34 (6)	0.35 (7)	0.5 (1)	1.00
7	90693	(d)	XPD	295	0.49 (1)	−0.65 (2)	−0.42 (4)	0.42 (4)	0.47 (4)	0.98
8	–	(e)	<i>Ab initio</i>	–	0.42	−0.71	−0.34	0.28	0.55	1.00
9	–	(f)	<i>Ab initio</i>	–	0.43	−0.679	−0.39	0.32	0.53	1.00
10	–	(g)	<i>Ab initio</i>	–	–	0.423	0.652	−0.448	−0.441	−0.91
11	–	(h)	<i>Ab initio</i>	–	–	0.52	0.573	−0.317	−0.549	−0.96

References: (a) Nemes & Kuhs (1985); (b) Glazer & Mabud (1978); (c) Shirane *et al.* (1955); (d) Joseph *et al.* (2000); (e) Garcia & Vanderbilt (1996); (f) Sághi-Szabó *et al.* (1998); (g) Ghosez *et al.* (1999); (h) Tinte *et al.* (2003).

where we separate its global amplitude Q from the internal form of the distortion \mathbf{e}^z , given by a normalized mode. This latter is the so-called ‘polarization vector’ of the distortion mode (Perez-Mato *et al.*, 2010), and it can be expressed as a linear combination of the normalized basis modes mentioned above. Hence, apart from the tetragonal strain of the unit cell, the structure is fully described by an amplitude Q (in units of ångström, because of the normalization used) and a four-dimensional normalized vector (c_1, c_2, c_3, c_4) .

The polar nature of the $P4mm$ phase implies that the structural models reported in the literature include, in general, an arbitrary global translation with respect to the cubic perovskite. For a meaningful comparison of different models, this arbitrary component of the distortion must be subtracted. According to the form of the basis modes $\{\varepsilon_1^z, \varepsilon_2^z, \varepsilon_3^z, \varepsilon_4^z\}$, a global translation along \mathbf{z} corresponds to a vector along the direction $(1, 1, 1, 2^{1/2})$ in this four-dimensional space. Thus, the component along this direction of any structure must be cancelled, which means enforcing the condition $c_1 + c_2 + c_3 + 2^{1/2}c_4 = 0$, in addition to the normalization condition $\sum_{i=1}^4 c_i^2 = 1$.

We have performed the symmetry-mode decomposition, in the form explained above, for various structures that have been reported for the $P4mm$ phase of PbTiO_3 . Table 2 summarizes the results. One can see the approximate invariance between the different models of the polarization vector describing the internal structure of the distortion mode, while the amplitude of the distortion can vary, as it is very sensitive to the temperature. The scalar product of the mode polarization vector (c_1, c_2, c_3, c_4) of each structure with that of Nemes & Kuhs (1985) (at 298 K, acting as reference) provides a quantitative value for the degree of their agreement. Notice that, for some of the structures listed in Table 2 (entries 10 and 11), the components of the mode polarization vector may have opposite signs. This corresponds to an equivalent twin-related structure. In the case of the experimental studies the agree-

ment is impressive, with the scalar product being unity up to the third or fourth digit. The only structure that differs considerably is that reported by Joseph *et al.* (2000), which is also the only one that was determined using X-ray diffraction. The rather important deviation of 0.02 of its scalar product is the result of the significant differences in the relative weights of the four basis modes.

The theoretical structures obtained as ground state from *ab initio* calculations (Garcia & Vanderbilt, 1996; Sághi-Szabó *et al.*, 1998) also exhibit a striking agreement with the experimental one, as shown by the coincidence of the mode polarization vectors. However, the distortion amplitude is smaller in the theoretical calculations. This is intriguing, since in general the amplitudes of *ab initio* calculated distortions tend to be larger than experimental ones, as in principle they correspond to its saturation value at 0 K. On the other hand, the *ab initio* calculated unstable polar phonon mode (Ghosez *et al.*, 1999; Tinte *et al.*, 2003) differs significantly from that present in the static equilibrium structure. In the latter, the Pb displacements have the greatest contribution, nearly double those of Ti. This is in fact a well known and distinctive feature of PbTiO_3 , in contrast with the case of BaTiO_3 , where the Ti displacements prevail over those of Ba. However, in the *ab initio* calculated unstable polar phonon modes, the weights of the Ti displacements are similar to or even larger than those of the Pb atoms. The reason for the significant deviation of the unstable dynamic phonon mode from the static distortion, determined both experimentally and in the *ab initio* calculations, is not clear. Although dynamic and static normal modes necessarily differ because of the atomic mass factors in the former, this difference is usually quite small. A more probable cause may be strong coupling with the tetragonal strain of the cell, or strong direct anharmonic couplings with the hard polar modes, which give these latter a significant weight in the relaxed structure. However, notice that the polar phonon modes calculated by the two *ab initio* calculations listed in

Table 3*P4mm* structural models of PZT.

The structures are each parameterized in terms of the amplitude of their polar distortion mode and the components of their polarization vector, as described in the text. The analogous decomposition of the structure of pure lead titanate reported by Nelmes & Kuhs (1985) is listed in the first row for comparison. The last column lists the scalar product of the polarization vector with that of Cox *et al.* (2005), which was taken as reference (entry 13). All models correspond to ambient conditions, except those explicitly indicated. For an explanation of the ICSD and Technique columns, see Table 2.

Entry	ICSD	Source	Technique	<i>x</i> Ti	Mode amplitude (Å)	Normalized polarization vector				e (153696)· e
						<i>c</i> 1	<i>c</i> 2	<i>c</i> 3	<i>c</i> 4	
1	61168	(a)	NSD	1.0	0.453 (1)	−0.703 (2)	−0.358 (4)	0.319 (3)	0.524 (4)	−0.96
2	90693	(b)	XPD	1.0	0.49 (1)	−0.65 (2)	−0.42 (3)	0.42 (4)	0.47 (4)	−0.92
3	90694	(b)	XPD	0.9	0.48 (1)	−0.66 (1)	−0.42 (2)	0.43 (3)	0.46 (3)	−0.92
4	90695	(b)	XPD	0.8	0.49 (1)	−0.65 (1)	−0.43 (2)	0.42 (3)	0.47 (3)	−0.91
5	90696	(b)	XPD	0.7	0.48 (1)	−0.66 (1)	−0.41 (2)	0.42 (3)	0.46 (3)	−0.91
6	90697	(b)	XPD	0.6	0.48 (1)	−0.65 (1)	−0.42 (2)	0.42 (4)	0.47 (3)	−0.91
7	90699	(b)	XPD	0.47	0.34	−0.81	−0.17	0.29	0.49	−0.91
8	90472	(c)	NPD	0.8	0.429 (6)	−0.74 (1)	−0.300 (4)	0.26 (2)	0.55 (3)	−0.99
9	90473	(c)	NPD	0.7	0.426 (9)	−0.74 (2)	−0.286 (6)	0.24 (3)	0.56 (4)	−0.99
10	90474	(c)	NPD	0.6	0.39	−0.76	−0.15	0.0	0.64	−0.98
11	90478	(c)	NPD	0.48	0.340 (4)	−0.85 (1)	−0.01 (5)	0.12 (3)	0.52 (3)	−1.00
12	93554	(d)	NPD	0.6 (10 K)	0.507	−0.657	−0.409	0.238	0.585	−0.95
13	153696	(e)	NPD	0.48 (325 K)	0.364 (4)	0.804 (8)	0.14 (2)	−0.16 (2)	−0.55 (2)	1
14	97059	(f)	NPD	0.48	0.41 (1)	0.77 (2)	0.24 (2)	−0.32 (5)	−0.49 (3)	0.98
15	183494	(g)	<i>Ab initio</i>	0.5	0.355	−0.778	−0.1661	0.099	0.597	−1.00

References: (a) Nelmes & Kuhs (1985); (b) Joseph *et al.* (2000); (c) Frantti *et al.* (2000); (d) Dmowski *et al.* (2001); (e) Cox *et al.* (2005); (f) Ragini *et al.* (2002); (g) Marton & Elsasser (2011).

Table 2 also differ considerably between themselves, and that of Tinte *et al.* (2003) was in fact a static mode calculation and included an optimized tetragonal strain.

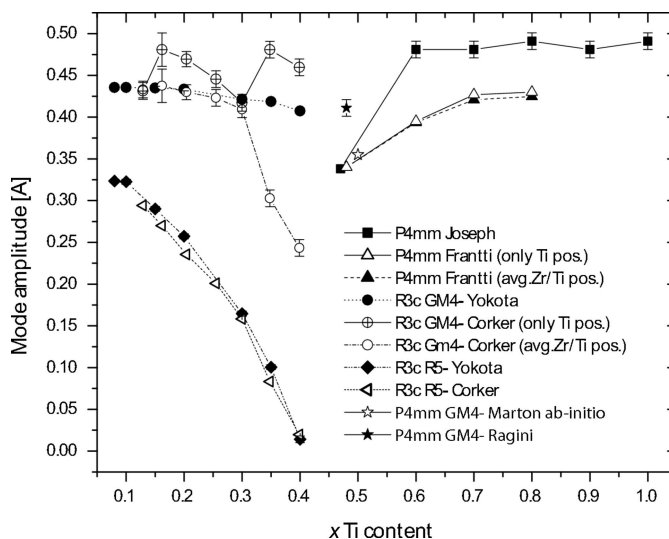
4. Tetragonal *P4mm* phase of Ti-rich PZT

A symmetry-mode analysis analogous to that for pure PbTiO_3 can be done for the tetragonal structures of PZT, which have been reported for various compositions. The results are summarized in Table 3 and Fig. 4. One can see that, according to the X-ray study of Joseph *et al.* (2000), except for the composition close to $x = 0.5$, the structure is essentially the same all along the x range (from 1 to 0.6). Both the amplitudes and the polarization vectors remain practically unchanged and equal to the values obtained for pure lead titanate using the same technique. However, these structures of Joseph *et al.* (2000) clearly differ from those obtained using neutron diffraction (see Table 2 and Fig. 4). Not only do the polarization vectors show strong discrepancies from those of the structures reported by Frantti *et al.* (2000) for similar compositions, but also the global amplitude of the polar distortion is significantly larger, as shown in Fig. 4. The origin of this systematic discrepancy is unclear, but it could be related to the expected lower accuracy in oxygen positions obtained with X-ray techniques. In any case, the structural models obtained by Frantti *et al.* (2000) in the composition range [0.8, 0.48] using neutron diffraction are much more consistent with the results for other compositions and other phases (see Table 3 and Fig. 4).

The structures reported by Frantti *et al.* (2000) were obtained by considering a split site for Zr and Ti. Table 3 lists the mode analysis obtained by considering Ti as the B site, the results obtained using the weighted average of the reported Ti

and Zr sites as the B site being very similar. The site splitting is so small that the results scarcely change (see Fig. 4).

Dmowski *et al.* (2001) also reported the PZT structure for $x = 0.6$ at 10 K (not shown in Fig. 4), which can be compared with those at room temperature for the same composition by Frantti *et al.* (2000) and Joseph *et al.* (2000). One can see in Table 3 that the amplitude of the polar mode is significantly larger, as one would expect at such a low temperature, but the mode polarization vector also differs considerably from that of the structure reported by Frantti *et al.* (2000), the Ti/Zr and O1 displacements having a much larger weight. In fact, the polarization vector is rather similar to that of Joseph *et al.* (2000) and therefore very close to that observed in pure lead

**Figure 4**

The amplitude of the polar distortion mode and the tilting mode (if it exists), plotted as a function of Ti content in the various structures reported for PZT under ambient conditions.

titanate, despite this being a neutron diffraction study. We have seen in the previous section that temperature is expected to influence strongly the global amplitude of the mode but not its polarization vector. Therefore, the reason for a change at low temperature to a polarization vector very similar to that of pure lead titanate is not clear, and this behaviour points to a possible aprioristic bias in the structure refinement.

Discarding the structure proposed by Joseph *et al.* (2000) for the reasons discussed above, there are four different tetragonal structures reported for compositions around $x = 0.5$. Three of them agree to a high degree. The mode amplitude varies among the models between 0.34 and 0.36 Å, while the mode polarization vectors essentially coincide [their scalar product with that of the structure reported by Cox *et al.* (2005) yields unity up to the second digit]. Only the structure proposed by Ragini *et al.* (2002) clearly deviates from the rest in both amplitude and mode polarization vector. The mode amplitude increases up to 0.41 Å and its polarization vector includes much larger displacements of the O1 atoms. These discrepancies can be considered strong and therefore make the model questionable. In view of its lower standard deviations and its essential agreement with the majority of the other models, we can consider the structure proposed by Cox *et al.* (2005) as the more reliable tetragonal structure for $x = 0.48$. Comparing this structure with the tetragonal structure of pure lead titanate, one observes a remarkable decrease in the distortion amplitude (see Fig. 4), while the weights of the Ti/Zr and O1 displacements in the polarization mode also decrease significantly, becoming rather marginal.

5. Rhombohedral phase of Ti-poor PZT

The rhombohedral phases in space groups $R3m$ or $R3c$ observed in the Ti-poor region of the phase diagram (see Fig. 1) contain a polar distortion also corresponding to the irrep $GM4^-$. While in the tetragonal phase the $GM4^-$ polar distortion takes the $[0, 0, 1]$ direction in the three-dimensional irrep space, in the rhombohedral phases it is along $[1, 1, 1]$. This means that the basis modes $\{\varepsilon_i^r\}$ with $i = 1-4$ that describe the distortion mode can be written in the form

$$\varepsilon_i^r = \frac{1}{3^{1/2}}(\varepsilon_i^x + \varepsilon_i^y + \varepsilon_i^z), \quad (2)$$

where the basis modes $\{\varepsilon_i^x, \varepsilon_i^y, \varepsilon_i^z\}$ are those described in §2 and Fig. 2. In terms of these rhombohedral basis modes, the $GM4^-$ structural distortion $Q\mathbf{e}^r$ given by the atomic displacements with respect to the cubic structure can be expressed in the form

$$Q\mathbf{e}^r = Q(c_1\varepsilon_1^r + c_2\varepsilon_2^r + c_3\varepsilon_3^r + c_4\varepsilon_4^r). \quad (3)$$

The normalized distortion mode \mathbf{e}^r (*i.e.* its polarization vector) can then also be expressed as

$$\mathbf{e}^r = \frac{1}{3^{1/2}}(\mathbf{e}^x + \mathbf{e}^y + \mathbf{e}^z), \quad (4)$$

where

$$\mathbf{e}^\alpha = c_1\varepsilon_1^\alpha + c_2\varepsilon_2^\alpha + c_3\varepsilon_3^\alpha + c_4\varepsilon_4^\alpha, \quad \alpha = x, y, z, \quad (5)$$

are three symmetry-equivalent polar distortions along the three main cubic axes. As both the rhombohedral phase and the tetragonal phases of PZT are in principle caused by a similar polar instability (*i.e.* an unstable threefold degenerate normal mode), the main difference between the two phases being the change of direction of the order parameter, one expects that the distortion modes $\{\mathbf{e}^x, \mathbf{e}^y, \mathbf{e}^z\}$ acting in the rhombohedral phase [equation (4)] are similar to those observed in the tetragonal phase, and therefore the components (c_1, c_2, c_3, c_4) in equation (3) are directly comparable with those of the tetragonal phase, which were discussed in the previous section. Furthermore, the global amplitude of the distortion should also be comparable, if the normalization condition is the same in both cases. Note that the program *AMPLIMODES* yields by default the mode amplitudes using the primitive unit cell of the distorted phase for the mode normalization. This means that the default mode amplitudes given by this program for the $R3c$ structures should be divided by a factor of $2^{1/2}$ to be comparable with those given for the tetragonal phase, as the rhombohedral phase has its primitive unit cell doubled with respect to the tetragonal one.

In the rhombohedral $R3c$ phase, a second irrep mode must be present besides the polar distortion. It doubles the unit cell, decreasing the symmetry from $R3m$ to $R3c$. It is a tilting mode of the O6 octahedra with wavevector $(\frac{1}{2}, \frac{1}{2}, \frac{1}{2})$ at the point R of the Brillouin zone. For the origin choice used here, its symmetry properties are given by the irrep $R5^-$. It involves a

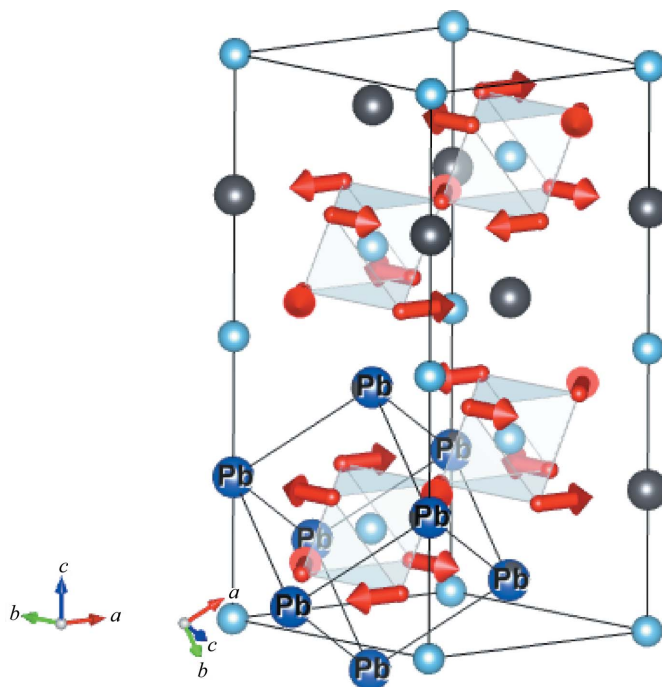


Figure 5 The $R5^-$ mode present in the $R3c$ phase of PZT, representing a tilting mode of the oxygen octahedra. It is fully defined by the irrep, having no freedom except its amplitude. For clarity, not all the interconnected oxygen octahedra are shown. This rigid unit mode of the O atoms multiplies the primitive unit cell by a factor of two.

Table 4

$R3c$ and $R3m$ structures of PZT, according to various experimental (NPD) reports.

The structures are parameterized in terms of the amplitude of its polar distortion mode $GM4^-$ and the components of its polarization vector, plus the amplitude of the $R5^-$ tilting mode. Structures with zero amplitude for the $GM5^-$ mode have $R3m$ symmetry ($R3c$ otherwise). The amplitudes are given (in ångström) with respect to the reference cubic structure described in §1. The amplitudes use the same normalization as in the tetragonal phase. The similarity of the distortion modes is checked through the scalar product of their polarization vector with entry 1, taken as reference. For an explanation of the ICSD and Technique columns, see Table 2.

Entry	ICSD	Source	x Ti	Temperature (K)	Mode amplitude		Normalized polarization vector				$e(1603)\cdot e$
					$GM4^-$	$R5^-$	c_1	c_2	c_3	c_4	
1	1603	(a)	0.1	293	0.41 (1)	0.278 (7)	0.81 (3)	0.10 (4)	−0.10 (1)	−0.57 (2)	1
2	1604	(a)	0.1	333	0.40 (1)	0.341 (8)	0.82 (4)	0.10 (4)	−0.14 (1)	−0.55 (2)	1.00
3	1605	(a)	0.1	373	0.34 (2)	0	0.82 (6)	0.10 (7)	−0.13 (1)	−0.55 (2)	1.00
4	1606	(a)	0.1	423	0.33 (2)	0	0.85 (7)	0.05 (7)	−0.20 (4)	−0.49 (4)	0.99
5	1607	(a)	0.1	473	0.23 (2)	0	0.82 (8)	0.13 (8)	−0.21 (2)	−0.52 (3)	0.99
6	1608	(a)	0.1	508	0.18 (5)	0	0.9 (3)	−0.1 (4)	−0.15 (6)	−0.4 (1)	0.9
7	86131	(b)	0.129	293	0.43 (1)	0.294 (5)	0.80 (2)	0.01 (2)	−0.066 (8)	−0.60 (2)	1.00
8	166424	(c)	0.1	293	0.44 (2)	0.324 (3)	0.790 (3)	0.124 (2)	−0.071 (5)	−0.596 (4)	1.00
9	46024	(d)	0.1	293	0.45 (3)	0.142 (8)	0.772 (7)	0.167 (6)	−0.276 (2)	−0.548 (3)	0.98
10	202844	(e)	0.25	83	0.44	0.26	0.81	0.09	−0.07	−0.58	1.00
11	202845	(e)	0.25	293	0.41	0.16	0.81	0.06	−0.06	−0.57	1.00

References: (a) Glazer *et al.* (1978); (b) Corker *et al.* (1998); (c) Yokota *et al.* (2009); (d) Ito *et al.* (1983); (e) Jiráček & Kala (1988).

single basis mode (shown in Fig. 5), and therefore this additional $R5^-$ distortion mode is fully determined by a single mode amplitude.

Table 4 and Fig. 4 summarize the results of the mode decomposition, as described above, for various rhombohedral structures reported for PZT in the region of low Ti content. One can see that, in general, the global amplitude of the $GM4^-$ distortion is similar to that observed in the tetragonal structure. The mode polarization vector, described by the four components (c_1 , c_2 , c_3 , c_4), essentially coincides in all models reported. Only the model of Ito *et al.* (1983) shows variations that are sufficiently significant to be pointed out. This model also clearly differs in the global amplitudes of both the polar and tilting modes, and its validity is therefore doubtful.

As expected, the polarization vector of the polar distortion in the $R3c$ or $R3m$ structures shown in Table 4 is quite consistent with that of the tetragonal phase in the Ti-rich range, listed in Table 3. For instance, the scalar product of the polarization vector present in the $x = 0.1$ $R3c$ structure reported by Glazer *et al.* (1978) at room temperature with that in the tetragonal phase from Nelmes & Kuhs (1985) (see Table 3) is 0.94. This is a rather good agreement, but not as high as those observed for different compositions and temperatures within the same phase. Comparing the two four-component vectors, one can see that the relative weights of the displacements of the Ti/Zr site and the O1 atom decrease considerably in the rhombohedral phase with respect to the tetragonal ones at larger x values, similar to what happens in the tetragonal structure for x around 0.5. In fact, the scalar product of the polarization vector in the rhombohedral structure given by Glazer *et al.* (1978) at room temperature for $x = 0.1$ with that of the tetragonal structure at $x = 0.48$ and 325 K proposed by Cox *et al.* (2005) is 0.99, demonstrating that the polar distortion in the rhombohedral phase does indeed involve essentially the same unstable mode observed around $x = 0.5$ in the tetragonal phase, but with a much larger amplitude. This mode decomposition consistency among many

of the different models obtained from various studies and for phases having different symmetries is non-trivial and represents significant evidence of their soundness, while putting into question those models that do not fulfill it.

The variation of the $R3c$ structure as a function of composition was studied by Corker *et al.* (1998) and Yokota *et al.* (2009). The amplitudes of the modes $GM4^-$ and $R5^-$ present in their structural models are depicted in Fig. 4. Concerning the octahedron-tilting mode $R5^-$, both studies yield a remarkable agreement, showing a strong x variation in its amplitude that decreases to zero around $x = 0.4$. Concerning the polar mode, the structures reported by Yokota *et al.* (2009) imply a weak and smooth variation in its global amplitude, demonstrating the self-consistency of the study. On the other hand, the structural models proposed by Corker *et al.* (1998) include a split Ti/Zr site, the Ti and Zr atoms having different positions. Fig. 4 shows for these split-site structural models the variation in the amplitude of the $GM4^-$ mode, taking a weighted average of the Zr and Ti positions, and also the result when the mode decomposition is done using only the Ti position. One can see that, in the first case, the variation in the mode amplitude essentially coincides with that in the Yokota *et al.* structures, while in the second case it fluctuates strongly. This noisy behaviour is also observed in the variation in the polarization vector, as shown by the strong variations in its scalar product with respect to the reference (see Fig. 6). This polarization vector scarcely changes with composition in the structure models of Yokota *et al.*, or in those of Corker *et al.* if they are modified by introducing a weighted average Zr/Ti site, while its variation acquires unacceptable fluctuations if the Ti position is considered. This confirms the assumption of Yokota *et al.* that models with a split Zr/Ti site introduce artefacts to the refinement.

The temperature variation in the amplitudes of the polar and tilting distortion modes, extracted from the rhombohedral structures reported by Glazer *et al.* (1978) for $x = 0.1$, is shown in Fig. 7. The magnitude of the polar distortion decreases as it

approaches the cubic phase, and from its fluctuations one can infer that the standard deviations obtained from the refinement clearly underestimate the uncertainties in the structural parameters. Although the structures at higher temperatures have $R3m$ symmetry, Glazer *et al.* (1978) described all of them within a common reference as $R3c$ structures. The actual higher symmetry of these $R3m$ structures is then reflected in the null amplitude of the $R5^-$ tilting mode when decomposed into irrep modes. As can be seen in Fig. 7, only the two structures at lower temperature have effectively $R3c$

symmetry, with a nonzero tilting mode. However, the increase in its amplitude from 298 to 333 K is strange, considering that it disappears at higher temperatures. Therefore, it would be worth reinvestigating this apparent anomalous behaviour experimentally, in the light of the results of the present mode analysis.

6. Monoclinic Cm phase

The direction within the irrep space of the $GM4^-$ order parameter in the monoclinic phase with symmetry Cm can be described by a normalized vector $(a/2^{1/2}, a/2^{1/2}, b)$, where a and b are free parameters under the constraint $a^2 + b^2 = 1$. This means that the $GM4^- Cm$ distortion Qe^m can be described in the form

$$Qe^m = Q(ae_{xy} + be_z), \tag{6}$$

in terms of a global amplitude and normalized modes along the z axis and in the xy plane. In the following we shall call (a, b) the ‘mode director’. The normalized mode e_z is necessarily a linear combination of the four basis modes $\{\varepsilon_i^z\}$ present in the tetragonal phase and described in §3,

$$e_z = c'_{1z}\varepsilon_1^z + c'_{2z}\varepsilon_2^z + c'_{3z}\varepsilon_3^z + c'_{4z}\varepsilon_4^z, \tag{7}$$

while the mode e_{xy} can be expressed as

$$e_{xy} = c'_{1xy}\varepsilon_1^{xy} + c'_{2xy}\varepsilon_2^{xy} + c'_{3xy}\varepsilon_3^{xy} + c'_{4xy}\varepsilon_4^{xy}, \tag{8}$$

with the basis normalized modes $\{\varepsilon_i^{xy}\}$ given by

$$\varepsilon_i^{xy} = \frac{1}{2^{1/2}}(\varepsilon_i^x + \varepsilon_i^y). \tag{9}$$

Here the modes $\{\varepsilon_i^x, \varepsilon_i^y\}$ are the basis modes along the x and y axes, analogous to $\{\varepsilon_i^z\}$.

According to the equations above, the description of the polar distortion in the monoclinic phase can be done in terms of eight basis modes:

$$GM4^- Cm \text{ distortion} = Q(c_{1xy}\varepsilon_1^{xy} + c_{2xy}\varepsilon_2^{xy} + c_{3xy}\varepsilon_3^{xy} + c_{4xy}\varepsilon_4^{xy} + c_{1z}\varepsilon_1^z + c_{2z}\varepsilon_2^z + c_{3z}\varepsilon_3^z + c_{4z}\varepsilon_4^z). \tag{10}$$

The amplitude Q and the eight components ($c_{1xy}, c_{2xy}, c_{3xy}, c_{4xy}, c_{1z}, c_{2z}, c_{3z}, c_{4z}$) of the polarization vector can be obtained using the program *AMPLIMODES*, although not necessarily ordered as above. Comparing with equations (6), (7) and (8), the values of the director (a, b) can be derived directly from these components, with

$$a = (c_{1xy}^2 + c_{2xy}^2 + c_{3xy}^2 + c_{4xy}^2)^{1/2} \tag{11}$$

and

$$b = (c_{1z}^2 + c_{2z}^2 + c_{3z}^2 + c_{4z}^2)^{1/2}. \tag{12}$$

If the monoclinic distortion were the result of the condensation of a single three-dimensional order parameter, the normalized mode e_{xy} would be such that $e_{xy} = (1/2^{1/2})(e_x + e_y)$, where e_x and e_y should be modes analogous to the observed mode e_z [equation (7)], but along the x and y axes, respectively. This would imply that the sets of components $(c'_{1xy}, c'_{2xy}, c'_{3xy}, c'_{4xy})$ and $(c'_{1z}, c'_{2z}, c'_{3z}, c'_{4z})$ must coincide. Thus,

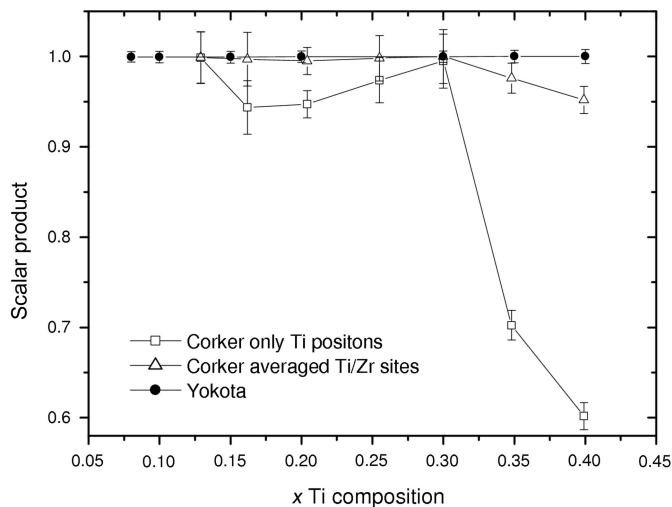


Figure 6 The scalar product of the polarization vector of the $GM4^-$ distortion, plotted as a function of composition according to the $R3c$ structures reported by Yokota *et al.* (2009) and Corker *et al.* (1998), using as reference that for $x = 0.4$ from Yokota *et al.* Only the structures reported by Yokota *et al.* for samples synthesized by the sol-gel method are included, the results being similar for the others. The structural models of Corker *et al.* include a split Ti/Zr site. The figure shows the results if an average position for this split site is considered and if, instead, the position of the Ti is used.

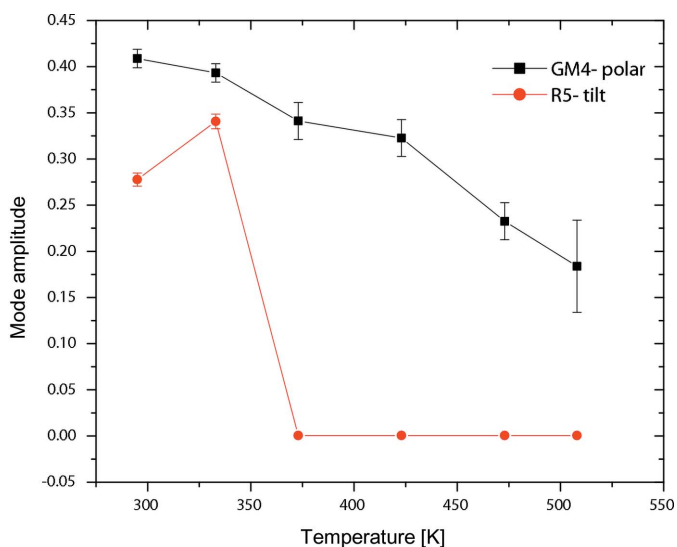


Figure 7 The amplitudes of the $GM4^-$ and $R5^-$ distortion modes in rhombohedral PZT with $x = 0.1$, plotted as a function of temperature according to the structures reported by Glazer *et al.* (1978). Zero amplitude of the $R5^-$ mode implies $R3m$ symmetry, and $R3c$ otherwise.

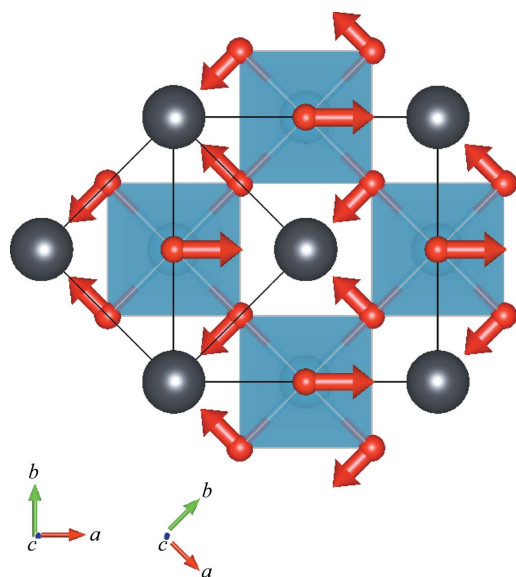
Table 5

Summary of the symmetry-mode decomposition of the Cm structures of PZT reported by Yokota *et al.* (2009) for different compositions, which were determined as a phase coexisting with the rhombohedral one.

The structures are each parameterized in terms of the amplitude of their polar distortion mode $GM4^-$, the components of the polarization vectors \mathbf{e}_{xy} and \mathbf{e}_z , the parameters (a , b), and the amplitude of the octahedral distortion mode $GM5^-$, as defined in the text. The amplitudes use the same normalization as in the tetragonal phase and the reference cubic structure described in §1. The similarity of the distortion modes is checked through the scalar product of their polarization vector with that of entry 7, which is taken as reference. The numbers in the ICSD row are deposition codes in the Inorganic Crystal Structure Database.

Entry	1	2	3	4	5	6	7
ICSD	166423	166425	166427	166429	166431	166433	166435
x Ti	0.08	0.1	0.15	0.2	0.3	0.35	0.4
$GM4^-$	0.474 (5)	0.428 (6)	0.393 (4)	0.392 (4)	0.393 (3)	0.382 (3)	0.382 (2)
$GM5^-$	0.087 (7)	0.05 (1)	-0.058 (7)	-0.041 (6)	-0.025 (5)	-0.028 (4)	-0.017 (4)
\mathbf{e}_{xy} , c'_{1xy}	0.870 (8)	0.87 (1)	0.797 (7)	0.806 (7)	0.783 (6)	0.812 (6)	0.817 (4)
c'_{2xy}	-0.39 (8)	-0.04 (3)	0.15 (1)	0.12 (1)	0.17 (1)	0.13 (1)	0.12 (1)
c'_{3xy}	-0.06 (8)	-0.16 (5)	-0.15 (3)	-0.12 (3)	-0.14 (1)	-0.18 (1)	-0.17 (1)
c'_{4xy}	-0.30 (8)	-0.47 (3)	-0.56 (3)	-0.57 (3)	-0.58 (1)	-0.54 (1)	-0.54 (1)
\mathbf{e}_z , c'_{1z}	0.735 (7)	0.77 (1)	0.794 (8)	0.811 (7)	0.812 (6)	0.838 (6)	0.854 (6)
c'_{2z}	0.207 (9)	0.18 (1)	0.11 (1)	0.08 (1)	0.08 (1)	0.04 (1)	-0.01 (1)
c'_{3z}	-0.03 (2)	-0.08 (2)	-0.07 (3)	-0.08 (3)	-0.09 (1)	-0.13 (1)	-0.12 (1)
c'_{4z}	-0.65 (2)	-0.61 (2)	-0.59 (3)	-0.58 (3)	-0.57 (1)	-0.53 (1)	-0.51 (1)
$\mathbf{e}_{xy} \cdot \mathbf{e}_z$	0.75	0.96	1.00	1.00	0.99	0.99	0.99
$\mathbf{e}(246565) \cdot \mathbf{e}$	0.82	0.92	0.99	0.99	0.99	1.00	1
Director (a , b)	(0.24, 0.97)	(0.39, 0.92)	(0.69, 0.73)	(0.67, 0.74)	(0.71, 0.70)	(0.68, 0.73)	(0.68, 0.73)
Director angle	76.10	67.03	46.61	47.84	44.6	47.03	47.03

we can say that a single-mode approximation or single-order-parameter approximation introduces a strong internal restriction on the form of the polar mode. In the real system, the presence of weaker secondary modes will break the rigorous fulfilment of this property, but one can expect that it will be approximately fulfilled. An internal correlation of this type should happen in any distorted structure of sufficiently low symmetry, such that the order parameter direction has some free parameter. This implies that, in these cases, as shown here for the Cm phase of PZT, the atomic displace-

**Figure 8**

The secondary $GM5^-$ mode allowed in the Cm phase of PZT. It is fully defined by the irrep, having no freedom except its amplitude. It produces a distortion of the oxygen octahedra and its amplitude is very small in all reliable structural models.

ments are expected to have approximate correlations that are beyond the framework of conventional crystallography.

The Cm structure of PZT allows a secondary nonpolar distortion mode with transformation properties given by the irrep $GM5^-$. This mode involves only oxygen displacements and represents a single degree of freedom, *i.e.* it is described by a single symmetry-determined basis mode (Fig. 8). As shown in Fig. 8, this mode produces a deformation of the octahedra, and its amplitude is expected to be very small.

In the literature, there are a variety of conditions and compositions for which the Cm phase has been observed for PZT. First, we consider the structures of Yokota *et al.* (2009), reported as coexisting with the rhombohedral phase down to very low Ti content. The results are summarized in Table 5. A summary of the mode analyses of other Cm structural models is given in Table 6. The components of the normalized vectors \mathbf{e}_{xy} and \mathbf{e}_z are listed in Table 5 for the structures of Yokota *et al.* (2009) only.

One can see in Table 5 that, with the exception of the two monoclinic structures of lower x values, the reported Cm structures as a function of composition reported by Yokota *et al.* (2009) fulfil the single-mode approximation up to a high degree. The variation in the two polarization vectors with x is very small, and the two normalized modes \mathbf{e}_{xy} and \mathbf{e}_z essentially coincide. This supports the soundness of the structures for $x > 0.1$. Their validity is also shown by the variation in the amplitudes of both $GM4^-$ and $GM5^-$ modes. Even though the latter is very weak, it shows a rather smooth variation. In contrast, the results of the mode decomposition of the two monoclinic structures determined for $x = 0.08$ and 0.1 differ considerably from the rest, and therefore these structures can be considered questionable. These monoclinic structures were determined by assuming their coexistence with a majority rhombohedral phase in proportions of 14.4 and 21.9% (Yokota *et al.*, 2009), respectively. It seems clear from the

Table 6

Summary of the symmetry-mode decomposition of various Cm structures of PZT.

The amplitudes use the same normalization as in the tetragonal phase and the reference cubic structure described in §1. The similarity of the distortion modes is checked through the scalar product of their polarization vector with entry 5, which is taken as reference. The Ti content is $x = 0.48$ in all cases, except for entry 9 where $x = 0.4$. For an explanation of the ICSD and Technique columns, see Table 2.

Entry	Source	ICSD	Conditions	Technique	Mode amplitude (Å)		$\mathbf{e}_{xy} \cdot \mathbf{e}_z$	$\mathbf{e}^m \cdot \mathbf{e}(153693)^m$	Director (a, b)	Director angle
					GM4 ⁻	GM5 ⁻				
1	(a)	246567	230 K	NPD	0.4122 (7)	0.007 (2)	0.99	1.00	(0.38, 0.92)	67.56
2	(a)	246568	280 K	NPD	0.4039 (8)	0.007 (2)	1.00	1.00	(0.37, 0.93)	68.3
3	(b)	51708	10 K	NPD	0.447 (5)	-0.021 (9)	0.98	0.99	(0.47, 0.88)	60.89
4	(b)	51707	295 K	NPD	0.393 (1)	-0.010 (4)	1.00	0.99	(0.26, 0.97)	75
5	(c)	153693	20 K	NPD	0.428 (3)	0.004 (7)	0.98	1	(0.46, 0.89)	62.67
6	(c)	153695	325 K	NPD	0.395 (6)	-0.01 (1)	1.00	0.99	(0.50, 0.87)	60.11
7	(d)	153676	10 K	NPD	0.43 (2)	0.14 (3)	0.91	0.9	(0.72, 0.69)	43.87
8	(e)	97060	295 K	XPD	0.74 (5)	-0.33 (7)	0.48	0.57	(0.84, 0.53)	32.25
9	(f)	166435	295 K	NPD	0.382 (2)	-0.017 (4)	0.99	0.91	(0.68, 0.73)	47.03

References: (a) Rouquette *et al.* (2005); (b) Frantti *et al.* (2001); (c) Cox *et al.* (2005); (d) Ranjan *et al.* (2005); (e) Ragini *et al.* (2002); (f) Yokota *et al.* (2009).

present analysis that such small proportions were insufficient for obtaining a meaningful structural model. Discarding these two structures of very low x , Table 5 shows that the monoclinic structures up to $x = 0.4$ reported by Yokota *et al.* (2009) satisfy the single-order-parameter approximation to a high degree. The study by Yokota *et al.* (2009), which reaches $x = 0.4$, shows not only that the atomic displacements in the xy plane and along the z axis follow patterns that are consistent with a single order parameter, but also that their combination, *i.e.* the parameters (a, b) defining the direction taken by the order parameter, remains essentially unchanged with composition. They satisfy approximately $a/b = 1$. This corresponds to a direction $(\frac{1}{2}, \frac{1}{2}, 1/2^{1/2})$ for the three-dimensional irrep polar mode, *i.e.* $(a, b) = (1/2^{1/2}, 1/2^{1/2}) = (0.707, 0.707)$, to be compared with the director $(a, b) = (2^{1/2}/3^{1/2}, 1/3^{1/2}) = (0.816, 0.577)$, associated with the order parameter direction $(1/3^{1/2}, 1/3^{1/2}, 1/3^{1/2})$ corresponding to the rhombohedral phase.

Table 6 shows that the situation is rather different for the Cm structural models reported for x around 0.5. There are two structures, namely those proposed by Ranjan *et al.* (2005) and Ragini *et al.* (2002), which clearly deviate from the single-order-parameter approximation. In both cases, and in contrast with the rest of the Cm models, the scalar product between \mathbf{e}_{xy} and \mathbf{e}_z deviates significantly from unity, even being less than 0.5 in the case of the work by Ragini *et al.* These two structural models also differ in the global amplitude of the distortion or in the magnitude of the secondary GM5⁻ distortion and will not be considered further. The remaining structures, obtained for $x = 0.48$, are all clearly consistent with the single-order-parameter approximation and very similar; their polarization vectors coincide to a high degree, while the global amplitude of the polar distortion is about 0.4 Å, similar to that in the neighbouring rhombohedral phase. The magnitude of the secondary GM5⁻ distortion is essentially negligible in all cases.

The director (a, b) describing the order parameter direction can also be compared among the various structures. Although this vector must have a considerable error, Fig. 9 shows that the directors of the various structures clearly concentrate

around the angle 64°. The directors of the different structures for $x = 0.48$ do not deviate from this angle by more than 4°, with the exception of the structure reported by Frantti *et al.* (2000) at room temperature. Fig. 9 also shows the directors concentrated around 45° for the Cm structures determined by Yokota *et al.* (2009) for $0.15 \leq x \leq 0.4$. Once the non-consistent structures are discarded, Fig. 9 shows that the order parameter director in the monoclinic phase around $x = 0.48$, where the piezoelectric response is a maximum, is rather equidistant between the tetragonal (90°) and the rhombohedral (~35.3°), confirming what has often been suggested as a probable feature of this phase.

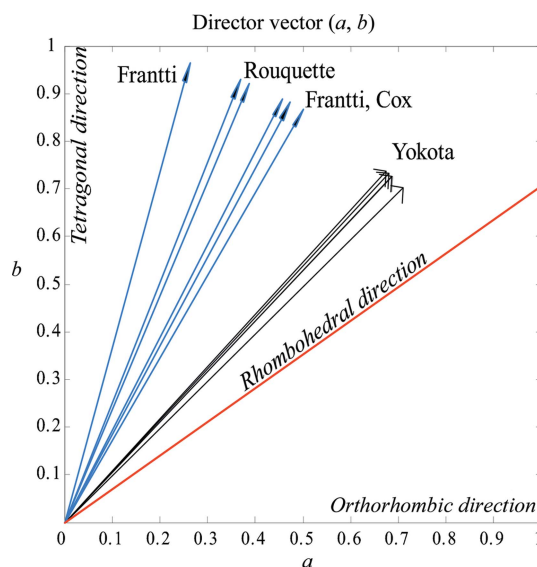


Figure 9 The director vector (a, b) describing the direction of the order parameter for the various Cm structures reported for $x = 0.48$ (see text). Structures that are not consistent with a single three-dimensional order parameter are not included. For comparison, the directors of the Cm structures reported by Yokota *et al.* (2009) for $0.15 \leq x \leq 0.4$ are also shown. The special directions corresponding to the rhombohedral, tetragonal and orthorhombic phases are indicated.

The results of Yokota *et al.* (2009) indicate that, although the monoclinic phase can be stabilized for other compositions, this optimum polarization orientation seems to be limited to the region around $x = 0.5$, and the order parameter director changes to orientations much closer to the rhombohedral phase for $x \leq 0.4$. It is important to stress that the direction of the order parameter in the monoclinic phase, represented by the director (a, b) , does not necessarily coincide with that of the ferroelectric polarization, but one can infer that they should be rather similar. In this context, it is interesting to remark that Rouquette *et al.* (2005) estimated the electric polarization using nominal ionic charges for their Cm structural models. Their calculated polarization deviates by about 19° from the tetragonal direction, compared with the approximate 22° deviation of the directors (a, b) obtained for these structures, listed in Table 6 and depicted in Fig. 9.

7. Monoclinic structure deduced from the rhombohedral one

The results above clearly demonstrate that secondary modes with the same symmetry as the order parameter, which may appear in the distorted phases as the result of high-order couplings, are very weak, such that the internal correlations of the polarization vector associated with a single-order-parameter distortion are well satisfied. This implies that, if this approximation is introduced *a priori*, one can obtain a good structural model for this phase from the symmetry mode analysis of another neighbouring or coexisting phase. More specifically, knowing the rhombohedral phase, one can have a good approximation of the atomic positions in the Cm phase, assuming that the three degenerate perovskite-unstable modes are the same, the monoclinic distortion being produced by a different combination of them, while its amplitude is similar. Only the director (a, b) has to be determined. More specifically, knowledge of the polarization vector of the polar mode and the mode amplitude in the rhombohedral phase enables one to obtain the values of the sets of components $(c'_{1xy}, c'_{2xy}, c'_{3xy}, c'_{4xy})$ and $(c'_{1z}, c'_{2z}, c'_{3z}, c'_{4z})$ in equations (8) and (7), respectively, defining the vectors \mathbf{e}_{xy} and \mathbf{e}_z , as they should coincide with the set of four components describing the mode polarization vector of the rhombohedral phase. Then, according to equation (6), if one assumes that the amplitude of the polar distortion is the same as in the rhombohedral phase, and the secondary distortion $GM5^-$ is negligible, only some choice for the director (a, b) is needed to construct a Cm monoclinic structure fully consistent with the polar distortion observed in the rhombohedral phase.

Table 7 compares a theoretical monoclinic structure constructed in this way with the experimental one. The monoclinic distortion was calculated from the rhombohedral structure reported by Yokota *et al.* (2009) for $x = 0.4$, and the comparison is done with the monoclinic structure reported by the same authors for this composition. To derive a monoclinic model from the rhombohedral one, a specific director (a, b) has to be assumed. For the comparison in Table 7 we have introduced the director derived from the experimental

Table 7

Theoretical Cm structure calculated from the knowledge of the coexisting rhombohedral phase, assuming that the distortion is produced by the same threefold degenerate polar mode.

The rhombohedral phase used for deriving this hypothetical monoclinic structure is that reported for $x = 0.4$ by Yokota *et al.* (ICSD 166434). For comparison, the monoclinic structure determined by the same authors for this composition (ICSD 166435) is given in parentheses. For the construction of the theoretical model, the director $(a, b) = (0.681, 0.732)$ was applied (see Table 5). The origin of the experimental structure has been shifted so that it does not include a global translation, similar to the theoretical one.

Atom	Site	x	y	z
Pb	$2a$	0.038 (0.0407)	0.0000	−0.050 (−0.0513)
Ti	$2a$	0.507 (0.4993)	0.0000	0.491 (0.4927)
O1	$2a$	0.480 (0.4808)	0.0000	0.007 (0.0108)
O2	$4b$	0.238 (0.2395)	0.243 (0.2455)	0.526 (0.5238)

monoclinic structure with which it is being compared (see Table 5). The agreement between theoretical and experimental models becomes obvious in this table. The maximum atomic shifts between the two models are of the order of 0.04 \AA , which should be compared with the maximum atomic displacements from the ideal cubic perovskite present in the monoclinic distortion, which are of the order of 0.35 \AA .

The comparison in Table 7 demonstrates that a constrained refinement of the monoclinic phase, applying restrictions resulting from the assumption of a single-mode distortion and with a significant reduction in the parameters to be fitted, can be an efficient approach for the determination of these phases. A conventional description of the Cm structure of PZT requires seven atomic positional parameters, which in the mode description correspond to the amplitudes of the two distinct irrep modes, plus the polarization vector of the polar mode. This last, although being defined by eight components, is subject to three equations (normalization, and zero global translations on the monoclinic plane), so that it reduces to five degrees of freedom. If the single-mode approximation is applied, the secondary mode $GM5^-$ is zero and the polarization vector of the polar distortion becomes simpler (see previous section), namely only two parameters are needed to define both vectors \mathbf{e}_{xy} and \mathbf{e}_z in equation (6). To define the atomic positions fully, only two additional parameters are then needed: the director (a, b) and the global amplitude of the mode.

Hence, the single-mode approximation reduces the number of adjustable positional parameters to four (only one more than for the tetragonal or rhombohedral phases). However if, in addition, the \mathbf{e}_{xy} and \mathbf{e}_z vectors are derived directly from the mode polarization vector present in a neighbouring rhombohedral or tetragonal phase, the additional parameters necessary to describe the monoclinic structure become only two. This constrained parameterization under the single-mode approximation can be especially efficient in the case of coexisting phases, as the addition of some proportion of monoclinic phase will imply a limited increase in the refinable parameters. Programs such as *FULLPROF* (Rodríguez-Carvajal, 1993) or *JANA2006* (Petříček *et al.*, 2006) have implemented new options that allow this type of mode-

Table 8

Summary of the symmetry-mode decomposition of the Cc structures reported for PZT at low temperature.

The Ti content is $x = 0.48$ in all cases, except for the last one where $x = 0.6$. The amplitudes (given in units of Å) use the same normalization as in the tetragonal phase and the reference cubic structure described in §1. The dimension of each mode (the number of degrees of freedom) is indicated in parentheses after its irrep label at the heading of each column. The numbers in the ICSD row are deposition codes in the Inorganic Crystal Structure Database.

Entry	ICSD	Source	Conditions	GM4 [−] (8)	GM5 [−] (1)	R5 ⁺ (1)	R3 [−] (1)	R4 [−] (2)	R5 [−] (2)
1	151354†	(a)	10 K	0.43 (7)	0.04 (1)	0	0.10 (1)	0	0.10 (1)
2	153675	(b)	10 K	0.436	0.023	0.059	0.021	0.012	0.199
3	153694	(c)	20 K	0.427	0.006	0	0.003	0	0.337
4	246565	(d)	47 K	0.435 (1)	0.003 (2)	0.056 (4)	0.014 (2)	0.061 (2)	0.115 (2)
5	246566	(d)	150 K	0.4206 (6)	0.000 (2)	0.057 (4)	0.014 (2)	0.048 (2)	0.089 (2)
6	246570	(d)	150 K/0.7 GPa	0.409 (3)	0.025 (6)	0.09 (1)	0.005 (7)	0.05 (7)	0.12 (8)
7	260167‡	(e)	4.1 GPa	0.303 (6)	0.03 (7)	0.02 (5)	0.04 (7)	0.053 (5)	0.14 (7)

† XPD data. ‡ $x(\text{Ti}) = 0.60$. References: (a) Pandey & Ragini (2003); (b) Ranjan *et al.* (2005); (c) Cox *et al.* (2005); (d) Rouquette *et al.* (2005); (e) Rouquette *et al.* (2008).

adapted refinement, where the parameters of a symmetry-mode description can be fitted directly and constrained if desired.

8. Monoclinic Cc phase

Hatch *et al.* (2002) showed that the correct symmetry of the low-temperature phase for compositions around $x = 0.5$ is Cc . There are a few structural models of this phase reported in the literature. Table 8 summarizes the mode decomposition of all these structures with respect to the reference cubic perovskite; only the amplitudes of the different irrep modes are listed. Apart from the expected polar GM4[−] mode and the R5[−] octahedral tilting modes, the Cc space group allows other degrees of freedom, represented by the additional irrep modes listed in the table. One can see that the amplitudes of these secondary modes are very small, typically one order of magnitude smaller than the prevailing polar distortion, and in many cases they are practically negligible, with their values being of the order of their standard deviations. One can infer that a model with these marginal modes set to zero beforehand, discarding five degrees of freedom out of a total of 13, would yield a structural model with similar reliability when fitted to the experimental data. In fact, when the different models are compared, the variation in these mode amplitudes is very high relative to their actual values. In contrast, the amplitude of the polar mode essentially agrees in all reported models for $x = 0.48$ under ambient conditions, being of the order of 0.43 Å, which is in fact an amplitude very similar to that in the Cm and rhombohedral phases. Only in the cases of structures determined at high pressures are these amplitudes significantly smaller, pressure being well known as a weakening agent of the polar distortion of these perovskites. In contrast, one can see in Table 8 that the amplitudes of the second primary distortion modes, corresponding to the octahedral tilting which is also present in the $R3c$ rhombohedral phase, vary strongly between the different models. The model of Cox *et al.* includes this R5[−] mode with an amplitude of 0.34 Å, while in the other models they are significantly smaller, being mostly of the order of 0.1 Å. The magnitude of this distortion is probably strongly dependent on the temperature,

but this does not seem to be sufficient to explain these strong discrepancies.

As we did with the Cm structures in the previous section, the internal single-mode consistency of the polar distortion GM4[−] can be crosschecked by expressing its polarization vector in terms of a director (a, b) and the pair of normalized four-dimensional modes \mathbf{e}_{xy} and \mathbf{e}_z , expressed in analogous bases. The results are summarized in Table 9. As in the case of the Cm structures, one can see that the single-mode approximation is satisfied extremely well. When expressed in an analogous mode basis, the normalized mode distortions in the xy plane and along \mathbf{z} of the reference cubic setting follow a very similar linear combination, quantified by the scalar product of the set of four components, represented in the column headed $\mathbf{e}_{xy}, \mathbf{e}_z$. In general, the linear combination of the corresponding four basis modes is very similar to those present in the monoclinic Cm phase or even in the tetragonal phase. One can, for instance, compare the values (−0.83, −0.03, 0.08, 0.55) for \mathbf{e}_{xy} in the Cc structure reported by Rouquette *et al.* (2005) for $x = 0.48$ and $T = 47$ K (Table 8) with (0.82, 0.12, −0.17, −0.54) for \mathbf{e}_{xy} in the Cm structure reported by Yokota *et al.* (2009) for $x = 0.4$ (Table 5), or with (−0.85, −0.01, 0.12, 0.52) for \mathbf{e}_z in the $P4mm$ structure reported by Frantti *et al.* (2000) for $x = 0.48$ (Table 3). The angle of the director (a, b) for the different models varies in the range 60–67°, *i.e.* a similar orientation of the order parameter as that underlying the Cm models of Frantti *et al.* (2001), Cox *et al.* (2005) and Rouquette *et al.* (2005) (see Fig. 9 and Table 6).

However, Table 9 also shows that the Cc structures reported at high pressure (last two entries) deviate significantly from the expected single-mode correlations. While the mode \mathbf{e}_z remains similar to that in the other models, the \mathbf{e}_{xy} distortion mode becomes completely different. For instance, the components of the Pb and Ti modes in the \mathbf{e}_{xy} distortion mode of the structure reported at 0.7 GPa are of the order of −0.68 and −0.33, respectively, compared with −0.83 and −0.04 at ambient pressure. This change is even more extreme at 4.1 GPa, where the values are −0.37 and −0.7, with the Ti-mode component prevailing. This extreme change in the \mathbf{e}_{xy} mode with pressure, while the \mathbf{e}_z mode remains essentially unchanged, is difficult to accept as a genuine effect of

Table 9

Components of the polarization vectors \mathbf{e}_{xy} and \mathbf{e}_z , and the order parameter director (a, b), as defined in the text, describing (except for an amplitude) the polar distortions present in the reported Cc structures of PZT (see Table 8).

The similarity of the vectors is checked through the scalar product of their four components. The second scalar product compares the total polar distortions of each model with that of the structure proposed by Rouquette *et al.* (2005) (entry 4). The two last entries are structures under pressure. The numbers in the ICSD row are deposition codes in the Inorganic Crystal Structure Database.

Entry	1	2	3	4	5	6	7
ICSD	151354†	153675	153694	246565	246566	246570	260167‡
$\mathbf{e}_{xy}, c'_{1xy}$	−0.76 (1)	−0.85	−0.86	−0.832 (2)	−0.825 (1)	−0.678 (6)	−0.372 (6)
c'_{2xy}	−0.3 (1)	−0.06	0.05	−0.03 (1)	−0.04 (1)	−0.33 (4)	−0.7 (1)
c'_{3xy}	0.26 (4)	0.26	0.09	0.083 (9)	0.07 (1)	0.10 (4)	0.14 (4)
c'_{4xy}	0.54 (6)	0.46	0.51	0.548 (9)	0.559 (9)	0.65 (2)	0.63 (6)
\mathbf{e}_z, c'_{1z}	−0.83 (1)	−0.82	−0.82	−0.798 (2)	−0.803 (1)	−0.816 (6)	−0.84 (1)
c'_{2z}	−0.07 (5)	−0.09	−0.12	−0.139 (5)	−0.133 (4)	−0.08 (2)	−0.01 (3)
c'_{3z}	0.15 (2)	0.12	0.17	0.128 (2)	0.138 (2)	0.098 (10)	0.12 (1)
c'_{4z}	0.53 (2)	0.56	0.54	0.572 (5)	0.565 (2)	0.56 (1)	0.52 (2)
$\mathbf{e}_{xy} \cdot \mathbf{e}_z$	0.97	0.98	0.98	0.99	0.79	0.96	0.67
$\mathbf{e}(246565) \cdot \mathbf{e}$	0.98	0.99	1	1	1	0.98	0.92
Director (a, b)	(0.52, 0.86)	(0.39, 0.92)	(0.46, 0.89)	(0.45, 0.89)	(0.43, 0.90)	(0.55, 0.84)	(0.50, 0.87)
Director angle (°)	58.84	67.03	62.67	63.18	64.46	56.78	60.11

† XPD data. ‡ $x(\text{Ti}) = 0.60$.

hydrostatic pressure. The reported structures exhibit strong deviations from the single-mode approximation; the threefold degeneracy of the underlying order parameter appears to break, which seems rather strange as an effect of an isotropic field. One may expect a change in the polarization vectors of the active polar modes, but keeping its threefold degeneracy, and therefore the approximate coincidence between the \mathbf{e}_{xy} and \mathbf{e}_z modes would be maintained. Being aware of the intrinsic difficulties of high-pressure experiments and their analysis, one may wonder if this asymmetry effect might rather be due to significant deviations from hydrostatic conditions or from the limitations of the data.

9. Conclusions

A survey of the various structures that have been reported for the different phases of PZT, as a function of composition and temperature, has been performed using their parameterization in terms of symmetry modes for a quantitative assessment and comparison. The study demonstrates that most of the published structural models comply to a high degree with the correlations expected in a structure resulting from a single three-dimensional order parameter. The mode decomposition allows a quantitative comparison of the different models, even those of different symmetries, demonstrating their basic agreement and consistency. One can deconvolute the variation in the global amplitudes of the different modes with temperature and composition from changes in the internal form of the modes, given by their polarization vectors, which are rather invariant and strongly correlated between the different phases. On the other hand, a few structures have been detected that do not fit within this approximation, and their discrepancies from the majority become patent. In particular, in the monoclinic Cm and Cc phases, it is shown that the action of a single order parameter for the polar distortion introduces a stringent subtle correlation of some atomic displacements in the xy plane with those along the z

direction. This correlation is fulfilled to a very good approximation by the majority of the reported structural models, while a strong deviation from this expected property is detected in some models. The mode parameterization has allowed the characterization the evolution of the polar order parameter, in both amplitude and direction, through the phase diagram of PZT.

Correlations between atomic displacements, beyond those forced by conventional crystallography, can be expected in any displacive distorted phase of sufficiently low symmetry such that the direction of its order parameter is not fully constrained by symmetry. This is the case in the monoclinic phases of PZT. The presence of weak secondary distortions will, in general, prevent these correlations from being exactly satisfied, but the present analysis shows that these subtle structural relations are fulfilled to a remarkably high degree. The agreement is so high that it can be conjectured that a structural model fulfilling them rigorously would fit the available data similarly well, the deviations being at the edge of the experimental resolution. This suggests that more efficient refinements of these difficult low-symmetry distorted pseudo-symmetric structures could be achieved by refining directly, instead of the atomic positions, the amplitudes of the symmetry basis modes constrained with the condition of representing a single-order-parameter distortion.

In addition, as the active three-dimensional order parameter polar distortion is essentially the same in all phases independent of their space-group symmetry, a first approximation to the structure of a particular phase can be derived from the knowledge of any other phase. For instance, a good approximation to the actual monoclinic Cm structure could be achieved from knowledge of the rhombohedral structure for a similar composition, using the same linear combination of basis modes observed in this phase and only changing the direction in the three-dimensional irrep space, to produce a corresponding global mode combination having Cm symmetry. These virtual Cm structures, constructed from

Table 10

Pairs of irreducible irreps that are interchanged when describing the transformation properties of a distortion mode of a structure with $Pm\bar{3}m$ symmetry, if the origin of the structure is shifted by $(\frac{1}{2}, \frac{1}{2}, \frac{1}{2})$.

Irreps standing alone remain invariant. Irrep labels follow the convention employed by *ISOTROPY* (Stokes *et al.*, 2007). The table has been crosschecked using the program *ISODISTORT* (Campbell *et al.*, 2006).

$R(\frac{1}{2}, \frac{1}{2}, \frac{1}{2})$	$(R1^+, R2^-)$	$(R2^+, R1^-)$	$(R3^+, R3^-)$	$(R4^+, R5^-)$	$(R5^+, R4^-)$	
$M(\frac{1}{2}, \frac{1}{2}, 0)$	$(M1^+, M4^+)$	$(M2^+, M3^+)$	$(M5^+)$	$(M1^-, M4^-)$	$(M2^-, M3^-)$	$(M5^-)$
$X(0, \frac{1}{2}, 0)$	$(X1^+, X3^-)$	$(X2^+, X4^-)$	$(X3^+, X1^-)$	$(X4^+, X2^-)$	$(X5^+, X5^-)$	

knowledge of the rhombohedral structure for a similar or equal composition, contain a single free parameter to be fitted, representing the freedom of the direction of the order parameter within the Cm subspace, and they agree with the reported Cm structure to a good approximation.

APPENDIX A

Dependence on the origin choice of the irrep labels of the modes

The mode analysis of PZT in this article has been done considering a description of the structure with the origin chosen such that atom Pb is at the origin while Zr/Ti is at $(\frac{1}{2}, \frac{1}{2}, \frac{1}{2})$ of the unit cell in a standard description of the $Pm\bar{3}m$ perovskite structure. An alternative description, which is frequently used, shifts the origin by $(\frac{1}{2}, \frac{1}{2}, \frac{1}{2})$, with the positions of the two cations interchanged and the oxygen coordinates varying accordingly. Both descriptions are of course equivalent and both use a standard setting for the space-group symmetry. However, the labelling of the active irrep modes unfortunately varies between the two descriptions. The reason for the non-invariance of the irrep labels associated with the modes is as follows.

Let us consider, for instance, an irrep that is even for the inversion operation $\{-1|, 0, 0, 0\}$. If the origin is shifted by $(\frac{1}{2}, \frac{1}{2}, \frac{1}{2})$, this operation becomes $\{-1|, -1, -1, -1\}$ when described using the new origin. This means that the irrep should now be even for this operation of the mathematical group, instead of the original one, $\{-1|, 0, 0, 0\}$. This may mean a different label for the irrep, as the irrep identification and its label depend on the transformations it assigns to the operations of the abstract mathematical group. This assignment must change if the origin is shifted and therefore the irrep label varies, although from the viewpoint of the structure the mode transformation properties described by the irrep are the same.

The label of an irrep of a given space group is the one that is also associated with its small irrep, *i.e.* an irrep of the small space group G_k , formed by the operations $\{\mathbf{R}|\mathbf{t}\}$ such that $\mathbf{R}\mathbf{k} = \mathbf{k}$ (modulo of a reciprocal lattice vector), where \mathbf{k} is the representative wave vector of the irrep. The small irrep associates with an operation $\{\mathbf{R}|\mathbf{t}\}$ a matrix of the form $\exp(i\mathbf{k}\cdot\mathbf{t})\mathbf{T}(\mathbf{R})$, where the set of matrices $\mathbf{T}(\mathbf{R})$ forms an irreducible (in general a projective) representation of the point group formed by the operations \mathbf{R} present in G_k (small co-

group). Thus, if an operation $\{\mathbf{R}|\mathbf{t}\}$ becomes $\{\mathbf{R}|\mathbf{t}'\}$ in the new description, the irrep should associate with this operation the same transformation matrix in both descriptions, and thus $\exp(i\mathbf{k}\cdot\mathbf{t}')\mathbf{T}'(\mathbf{R}) = \exp(i\mathbf{k}\cdot\mathbf{t})\mathbf{T}(\mathbf{R})$, where $\mathbf{T}'(\mathbf{R})$ is the matrix associated with \mathbf{R} by the small irrep of the small co-group in the second description. The irrep $\mathbf{T}'(\mathbf{R})$ determines the label of the irrep in the second description. For instance, in the example above, if $\mathbf{k} =$

$(\frac{1}{2}, \frac{1}{2}, \frac{1}{2})$ (point R in the Brillouin zone), the matrix associated with $\{-1|, -1, -1, -1\}$ is $\exp(i\pi)\mathbf{T}'(-1)$ and this should be equal to $\mathbf{T}(-1)$.

Thus, if T is even for the inversion, \mathbf{T}' must be odd, and all irreps at the R point assigned to the distortion modes change parity for inversion if the origin of the structure is shifted by $(\frac{1}{2}, \frac{1}{2}, \frac{1}{2})$. According to the general equation above, the same happens for X irreps $[\mathbf{k} = (0, \frac{1}{2}, 0)]$, while the parity is conserved for the point M $[\mathbf{k} = (\frac{1}{2}, \frac{1}{2}, 0)]$. Similarly, the necessary changes for the other operations of the small co-group can be determined and the pairs of irreps that are necessarily interchanged by the origin shift can be derived. For further (probably useful) reference, Table 10 lists, for the three symmetry points of the Brillouin zone of $Pm\bar{3}m$, the set of pairs of irreps that are interchanged by the origin shift.

This work was supported by the Basque Government (project No. IT779-13) and the Spanish Government (project No. MAT2012-34740). BK thanks the Lifelong Learning Leonardo da Vinci programme of the European Commission for financial support. EST acknowledges support from TUBITAK through the 2232 programme.

References

Aroyo, M. I., Kirov, A., Capillas, C., Perez-Mato, J. M. & Wondratschek, H. (2006). *Acta Cryst.* **A62**, 115–128.
 Aroyo, M. I., Perez-Mato, J. M., Capillas, C., Kroumova, E., Ivantchev, S., Madariaga, G., Kirov, A. & Wondratschek, H. (2006). *Z. Kristallogr.* **221**, 15–27.
 Aroyo, M. I., Perez-Mato, J. M., Orobengoa, D., Tasci, E., De La Flor, G. & Kirov, A. (2011). *Bulg. Chem. Commun.* **43**, 183–197.
 Campbell, B. J., Stokes, H. T., Tanner, D. E. & Hatch, D. M. (2006). *J. Appl. Cryst.* **39**, 607–614.
 Corker, D. L., Glazer, A. M., Whatmore, R. W., Stallard, A. & Fauth, F. (1998). *J. Phys. Condens. Matter*, **10**, 6251–6269.
 Cox, D. E., Noheda, B. & Shirane, G. (2005). *Phys. Rev. B*, **71**, 134110.
 Dmowski, W., Egami, T., Farber, L. & Davies, P. K. (2001). *AIP Conf. Proc.* **582**, 33–44.
 Frantti, J. (2008). *J. Phys. Chem. B*, **112**, 6521–6535.
 Frantti, J., Lappalainen, J., Eriksson, S., Ivanov, S., Lantto, V., Nishio, S., Kakihana, M. & Rundlöf, H. (2001). *Ferroelectrics*, **261**, 193–198.
 Frantti, J., Lappalainen, J., Eriksson, S., Lantto, V., Nishio, S., Kakihana, M., Ivanov, S. & Rundlöf, H. (2000). *Jpn. J. Appl. Phys.* **39**, 5697–5703.
 Garcia, A. & Vanderbilt, D. (1996). *Phys. Rev. B*, **54**, 3817–3824.
 Ghosez, Ph., Cockayne, E., Waghmare, U. V. & Rabe, K. M. (1999). *Phys. Rev. B*, **60**, 836–843.
 Glazer, A. M. & Mabud, S. A. (1978). *Acta Cryst.* **B34**, 1065–1070.
 Glazer, A. M., Mabud, S. A. & Clarke, R. (1978). *Acta Cryst.* **B34**, 1060–1065.

- Hatch, D. M., Stokes, H. T., Ranjan, R., Ragini, X., Mishra, S. K., Pandey, D. & Kennedy, B. J. (2002). *Phys. Rev. B*, **65**, 212101.
- Ito, H., Shiozaki, Y. & Sawaguchi, E. (1983). *J. Phys. Soc. Jpn.*, **52**, 913–919.
- Jaffe, B., Jaffe, H. L. C. & Cook, W. R. (1971). *Piezoelectric Ceramics, Non-metallic Solids*. New York: Academic Press.
- Jirák, Z. & Kala, T. (1988). *Ferroelectrics*, **82**, 79–84.
- Joseph, J., Vimala, T. M., Sivasubramanian, V. & Murthy, V. R. K. (2000). *J. Mater. Sci.* **35**, 1571–1575.
- Lines, E. & Glass, A. M. (1977). *Principles and Applications of Ferroelectrics and Related Materials*. Oxford University Press.
- Marton, P. & Elsasser, C. (2011). *Phys. Status Solidi B*, **248**, 2222–2228.
- Nelmes, R. J. & Kuhs, W. F. (1985). *Solid State Commun.* **54**, 721–723.
- Orobengoa, D., Capillas, C., Aroyo, M. I. & Perez-Mato, J. M. (2009). *J. Appl. Cryst.* **42**, 820–833.
- Pandey, D. & Ragini, R. (2003). *Z. Kristallogr.* **218**, 1–7.
- Perez-Mato, J. M., Orobengoa, D. & Aroyo, M. I. (2010). *Acta Cryst.* **A66**, 558–590.
- Petríček, V., Dušek, M. & Palatinus, L. (2006). *JANA2006*. Institute of Physics, Czech Academy of Sciences, Prague, Czech Republic.
- Ragini, R., Ranjan, R., Mishra, S. K. & Pandey, D. (2002). *J. Appl. Phys.* **92**, 3266–3274.
- Ranjan, R., Singh, A. K., Ragini, R. & Pandey, D. (2005). *Phys. Rev. B*, **71**, 092101.
- Rodríguez-Carvajal, J. (1993). *Physica B*, **192**, 55–69.
- Rouquette, J., Haines, J., Bornand, V., Pintard, M., Papet, Ph., Marshall, W. G. & Hull, S. (2005). *Phys. Rev. B*, **71**, 024112.
- Rouquette, J., Haines, J., Fraysse, G., Al-Zein, A., Bornand, V., Pintard, M., Papet, Ph., Hull, S. & Gorelli, F. A. (2008). *Inorg. Chem.* **47**, 9898–9904.
- Sághi-Szabó, G., Cohen, R. E. & Krakauer, H. (1998). *Phys. Rev. Lett.* **80**, 4321–4324.
- Shirane, G., Pepinsky, R. & Frazer, B. C. (1955). *Phys. Rev.* **97**, 1179–1180.
- Stokes, H. T., Hatch, D. M. & Campbell, B. J. (2007). *ISOTROPY*, <http://stokes.byu.edu/iso/isotropy.php>.
- Tinte, S., Rabe, K. M. & Vanderbilt, D. (2003). *Phys. Rev. B*, **68**, 144105.
- Woodward, D. I., Knudsen, J. & Reaney, I. M. (2005). *Phys. Rev. B*, **72**, 104110.
- Yokota, H., Zhang, N., Taylor, A. E., Thomas, P. A. & Glazer, A. M. (2009). *Phys. Rev. B*, **80**, 104109.
- Yokota, H., Zhang, N., Thomas, P. A. & Glazer, A. M. (2011). *Ferroelectrics*, **414**, 147–154.